
EVALUATING WEATHER FORECASTS FROM A DECISION MAKER'S PERSPECTIVE

Kornelius Raeth* Nicole Ludwig

University of Tübingen
Tübingen AI Center
Germany

Corresponding author: Kornelius Raeth
kornelius.raeth@uni-tuebingen.de

ABSTRACT

Standard weather forecast evaluations focus on the forecaster's perspective and on a statistical assessment comparing forecasts and observations. In practice, however, forecasts are used to make decisions, so it seems natural to take the decision-maker's perspective and quantify the value of a forecast by its ability to improve decision-making. Decision calibration provides a novel framework for evaluating forecast performance at the decision level rather than the forecast level. We evaluate decision calibration to compare Machine Learning and classical numerical weather prediction models on various weather-dependent decision tasks. We find that model performance at the forecast level does not reliably translate to performance in downstream decision-making: some performance differences only become apparent at the decision level, and model rankings can change among different decision tasks. Our results confirm that typical forecast evaluations are insufficient for selecting the optimal forecast model for a specific decision task.

1 Introduction

Weather forecasts have a daily impact on people's lives by providing early warnings of extreme events and guiding decision-making in critical industries like aviation, public health, agriculture and energy. With climate change intensifying weather extremes, accurate forecasts are increasingly important. Recently, Machine Learning weather prediction (MLWP) models (Lam et al., 2023; Lang et al., 2024a; Chen et al., 2023) are rivaling or surpassing performance of classical numerical weather prediction (NWP) models across many metrics and variables. However, deterministic point forecasts hide the uncertainty inherent in weather prediction due to atmospheric stochasticity and modeling limitations, making uncertainty quantification essential for forecast validity (Murphy, 1993; Palmer, 2019). To address this, ensemble forecasts were introduced into NWP systems (Palmer et al., 1993). Probabilistic MLWP models have recently achieved performance comparable to traditional numerical models (Price et al., 2023; Lang et al., 2024b; Couairon et al., 2024; Bonev et al., 2025). From a forecaster's perspective, a good probabilistic forecast should be maximally sharp while remaining calibrated (Gneiting et al., 2007). Sharp forecasts have low variance. Calibration refers to the statistical consistency between forecasts and observations (e.g., a 90% prediction interval derived from the forecast should cover the observation 90% of the time). But are those really the key properties of a forecast that are relevant to end users who use forecasts to make decisions?

Good forecasts improve decision-making Ultimately, forecasts are used to make decisions and the value of a forecast lies in its ability to improve decision-making (Sweeney et al., 2020; Zhu et al., 2002; Murphy, 1994). Yet, typical forecast evaluations only consider the forecaster's perspective and ignore downstream decision tasks (Maciejowska et al., 2025). In theory, forecasts fulfilling distribution calibration (Song et al., 2019) yield optimal downstream decisions. However, distribution calibration represents a strong notion of calibration that is difficult to attain and verify in practice

*This work was supported by the DFG – EXC number 2064/1 – Project number 390727645 and by the German Federal Ministry of Research, Technology and Space (BMFTR) through the FEAT project (grant number 16IS22073A).

(Zhao et al., 2021; Sahoo et al., 2021). While weaker forms of calibration can be achieved and validated, they typically offer no guarantees for improved decision-making. Common diagnostic tools for calibration in weather forecasting involve probability integral transform (PIT) histograms, proper scoring rules like the continuous ranked probability score (CRPS) (Gneiting et al., 2007) and spread skill ratios (SSR) (Fortin et al., 2014). While all of them quantify some form or aspect of calibration, they may omit forecast properties relevant to decision-making (Murphy, 1993). This highlights the need to evaluate calibration from the decision-maker’s perspective, at the level of decisions rather than forecasts.

Calibration as precise cost estimation Decision tasks can be modeled via cost functions of actions and observations. Forecasts are then used to estimate costs and make decisions. In this setup, calibration is framed as precise cost estimation (Derr et al., 2025): a forecast is considered calibrated if it correctly anticipates the costs of a particular action (expected cost = observed cost). This notion is called decision calibration (Zhao et al., 2021) and shifts evaluation focus from distribution matching to only those forecast properties relevant for the specific decision task.

Contributions We present the first study to evaluate the performance of state-of-the-art weather forecasting models for downstream decision-making using the decision calibration framework.

- We evaluate performance on decision tasks from three core weather-dependent sectors: agriculture, civil protection and renewable energy operation.
- We investigate to what extend calibration performance at the forecast level translates into performance in downstream decision-making.
- We compare state-of-the-art numerical and ML weather prediction models with respect to decision calibration.

Related work Existing work on decision calibration primarily focuses on medical applications (disease detection, hospital acceptance) (Zhao et al., 2021; Sahoo et al., 2021). Studies on the value of weather forecasts investigate the relative economic value (REV) of ensemble forecasts (Zhu et al., 2002; Richardson, 2000; Price et al., 2023) considering simple cost-loss ratio decision tasks. However, REV analyses only consider incurred costs, not decision calibration. In contrast, we perform our analysis within the more general decision calibration framework, which accommodates any cost function and action space while considering both anticipated and incurred costs.

2 Decision-making and calibration

2.1 Setup and notation

We consider a regression task where the goal is to learn a mapping from input features $X \in \mathcal{X} \subset \mathbb{R}^m$ to targets $Y \in \mathcal{Y} \subset \mathbb{R}$, where X, Y are random variables and distributed according to a data generating process $P_{X,Y}$. We are interested in probabilistic modeling, so given an input X , we write F_X to denote the predictive cumulative distribution function (CDF) over targets \mathcal{Y} that ideally recovers the true CDF of $Y|X$.

2.2 Optimal decision-making under uncertainty

In the context of optimal decision-making, predictions are used to take actions from an action space \mathcal{A} that minimize expected costs. To formalize this, consider a cost function $c : \mathcal{A} \times \mathcal{Y}$, that quantifies the cost $c(a, y)$ incurred by a decision maker when taking action $a \in \mathcal{A}$ and observing $y \in \mathcal{Y}$. Given a probabilistic prediction F_x over \mathcal{Y} , the Bayes decision rule δ_c selects the action that yields the minimal expected costs under F_x

$$\delta_c(F_x) := \arg \min_{a \in \mathcal{A}} \mathbb{E}_{Y \sim F_x} [c(a, Y)]. \quad (1)$$

2.3 Decision calibration

Decision calibration (Zhao et al., 2021) holds when the expected costs (of the optimal action) under the forecast match with the true observed costs. The cost gap is the absolute difference between the two and a measure of decision (mis-) calibration. More precisely, the expected cost of the optimal action under the forecast is given by

$$C_{exp} = \mathbb{E}_X \mathbb{E}_{\hat{Y} \sim F_X} [c(\delta_c(F_X), \hat{Y})] \quad (2)$$

and can be seen as a simulation of the incurred costs. The observed costs are given by

$$C_{obs} = \mathbb{E}_{X,Y} [c(\delta_c(F_X), Y)] \quad (3)$$

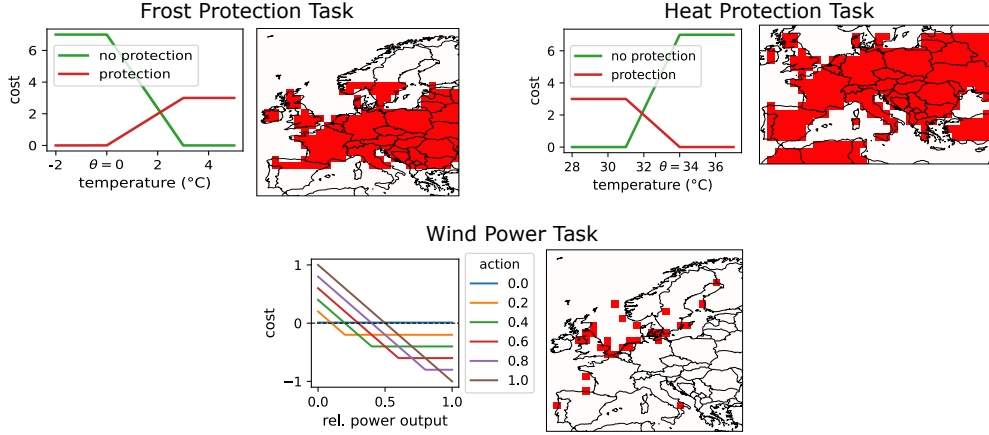


Figure 1: Cost functions and evaluated grid points (red) for the frost protection task, heat protection task ($c = 0.7$), and wind power task ($u_{\text{pen}} = 2$). For visual clarity, we only plot costs for every other action in the wind power task.

and measure the actual costs after observing the true values of Y . The cost gap is given by

$$C_{\text{gap}} = |C_{\text{exp}} - C_{\text{obs}}| \quad (4)$$

with $C_{\text{gap}} = 0$ for perfect decision calibration.² In a good forecast both cost gap and observed cost should be small: forecasts should correctly anticipate the incurred costs but also lead to small incurred costs, i.e. good decisions.

A cost function associated with a decision task translates the abstract concept of uncertainty in probabilistic forecasts into an interpretable and actionable quantity: the expected cost of a particular action. The expectation automatically accounts for the fact that even low probability events can have a high impact if they are costly. Different cost functions require calibration in different parts of \mathcal{Y} to enable good decisions. In some subsets $\bar{\mathcal{Y}} \subset \mathcal{Y}$ decisions may be trivial (e.g., when $c(a_0, y) < c(a_1, y) \forall y \in \bar{\mathcal{Y}}$) and calibration is unnecessary. However, in parts where $c(a_0, \cdot)$ and $c(a_1, \cdot)$ cross, good calibration is essential to correctly estimate expected costs and make optimal decisions. Thus, cost functions encode user-specific costs and preferences, enforcing calibration only where it matters for the decision task.

3 Weather forecasts and decision-making

Weather forecasts are used for decision-making so it seems natural to evaluate their performance at the level of decisions rather than at the level of forecasts. Weather forecasting is therefore predestined for a decision calibration analysis. In the following we introduce and motivate weather related decision tasks and explain how decision calibration is evaluated.

3.1 Decision tasks

There are many decision tasks related to weather, yet we were unable to find any that have already been translated into a cost function. Therefore, we define our own cost functions for decision tasks from three core weather-dependent sectors (da Silva et al., 2025; Farkas et al., 2025): agriculture (Calanca et al., 2011), civil protection (Hughes et al., 2004; Sol, 1994) and renewable energy management (Meenal et al., 2022; Sweeney et al., 2020). We keep the cost functions as simple as possible while remaining realistic for the task at hand, and simulate a Bayes decision-making process.

Agriculture Yields and losses in agriculture are strongly affected by weather. We focus on the effects of low temperatures on crop yield. When temperatures drop too low, plants die, causing crop and economic losses (Snyder and Melo-Abreu, 2005). In the US, frost causes the biggest economic damage among all meteorological events (Juurakko et al., 2021; White and Haas, 1975). Farmers, therefore, need to decide whether to employ frost protection measures (covering plants, active heating, or early harvesting) when freezing temperatures are likely Snyder and Melo-Abreu (2005). These measures are costly and should only be applied when necessary. We model a binary decision task, whether to apply frost protection, defining a threshold temperature θ below which the plants die ($t_{\text{obs}} \leq \theta$) and consider

²The expectation over X does not need to be taken over the whole domain \mathcal{X} but instead can be over subsets of \mathcal{X} or in the extreme case individual $x \in \mathcal{X}$, leading to stronger conditions than the mere equivalence of average expected and true costs.

them safe if $t_{obs} \geq \theta + 3$. Without protection, we incur the maximum cost (all crops are lost) when plants die, and no cost when they are safe. For intermediate temperatures, we interpolate linearly. With protection, we flip the cost function: incurring a cost when protection is unnecessary and no cost when it saves the crop. We use asymmetric costs, where the cost ratio $c \in (0, 1)$ weights costs of missed protection ($c \cdot 10$) and unnecessary protection $(1 - c) \cdot 10$, see Figure 1. Varying θ and c allows us to model decision tasks for plants with different temperature sensitivities and protection costs. We evaluate on Europe for 00 UTC forecasts, considering mid-latitudes where agriculture and frost are likely.

Civil protection Extreme weather events like heavy rain or snowfall, floods and heatwaves can pose a serious threat to the population. Since the frequency of extreme events is expected to increase as a result of climate change, reliable early warning systems become more relevant (Eriksen et al., 2023). We focus on heat events, responsible for high numbers of heat-related illnesses and deaths every year. Heat-related deaths can be prevented, for instance by protecting vulnerable groups, but the protective measures require early warning systems to be effective (Luber and McGeehin, 2008; Meerow and Keith, 2022; Hess et al., 2023). However, heat protection measures come at a cost and should therefore only be put in place when required. We model a binary decision task, whether to apply heat protection, using the same cost function design as in the frost protection task above, but with θ now marking the temperature of maximum heat-related cost (see Figure 1). For larger θ , the decision task is moved into the tails of the distribution. We vary θ and cost ratio c to cover multiple tasks (sensitivities and costs) and evaluate performance in Europe for 12 UTC forecasts, excluding Scandinavia.

Renewable energy management The availability of renewable energy sources such as wind and solar energy depends on the weather. A large-scale expansion of renewable energy therefore requires forecasts that can reliably predict their availability so that dispatch plans can be made to ensure power system stability (Botterud et al., 2011; Sweeney et al., 2020). In the case of wind power, this leads to a dispatch decision task, where a wind power provider needs to decide in advance how much power he will provide at some point in the future and deviations from the guaranteed amount can lead to punishments Bourry et al. (2008). We model this as a multi-action decision task, where each action corresponds to a particular amount of relative power that the provider promises to deliver (see Figure 1). We consider 11 actions where 10 actions partition the relative power space into equal size bins (0.1, 0.2, ..., 1.0). The more energy the provider promises, the more he gets paid. However, in the case of a production deficit, he needs to account for the missing amount by buying (expensive) energy from other sources which increases his costs (linear cost punishment). In the case of a production surplus, wind farms can reduce the power output (curtailment) to not exceed the target amount, hence, no penalty costs apply (Bruninx et al., 2025). In this case, however, the provider would have been better off by predicting a higher power output. We model such opportunity costs implicitly through the (lower) cost of other actions. Additionally, there is a ‘turbine-off’ action with a very small constant cost (standby drain) when no power is expected due to low or too high wind speeds. We evaluate performance on grid points in Europe with offshore wind farms³ for 00 UTC forecasts. We vary the penalty for under-delivering by changing the slope of the cost function (u-pen). We use the power law to extrapolate wind speeds from 10 meters to turbine hub height, then convert to wind power using a standard power curve; for details see section A.1.

3.2 Weather prediction models

We consider a standard numerical weather prediction model and a novel machine learning weather prediction model. The IFS ENS is the probabilistic NWP model operational at the European Center for Medium-Range Weather Forecasts (ECMWF) that provides ensemble forecasts. Each ensemble member is generated by running the numerical solver with slightly perturbed initial conditions and physical parameters leading to different forecasts. For the MLWP model we use ArchesweatherGen (Couairon et al., 2024), a generative ML weather prediction model that provides probabilistic weather forecasts. We will refer to it as Arches from now on. Arches is based on a diffusion model (Ho et al., 2020) that is trained to learn the true data distribution based on the training data. Once trained, the model can generate samples from the learned forecast distribution (for 24 h lead time) given the two past states of the atmosphere. Forecasts with longer lead times are obtained through autoregressive rollouts.

3.3 Evaluating decision calibration of weather forecasts

In weather forecasting we input the state of the atmosphere at time t , X_t and aim to predict the state of the atmosphere at lead time l , X_{t+l} . Let Y_{t+l} denote the weather variable of interest (e.g., 2 meter temperature) extracted from X_{t+l} . We evaluate ensemble forecast models, that provide M samples from the forecast distribution $F_{X_t}^l$

$$\{\hat{Y}_{t+l}^{(i)}\}_{i=1}^M \sim F_{X_t}^l. \quad (5)$$

³Dataset on offshore wind farms provided by the European Marine Observation and Data Network (EMODnet).

We approximate the expected costs in Eq. (1) via a Monte Carlo estimate

$$\mathbb{E}_{\hat{Y}_{t+l} \sim F_x^l} [c(a, \hat{Y}_{t+l})] \approx \frac{1}{M} \sum_{i=1}^M c(a, \hat{Y}_{t+l}^{(i)}). \quad (6)$$

We consider single surface variables, hence for every lead time, grid point and day of the year we obtain an ensemble forecast and a corresponding observation. Given a particular decision task, we compute the expected cost for every ensemble forecast and compare it to the observed cost using the corresponding observation to obtain the cost gap. That is, we compute the cost gap for every observation individually instead of first averaging costs over observations as in Eq.(2). We do this because average cost comparisons can mask poor performance of individual forecast instances, as discussed in Zhao et al. (2021). After computing the cost gap and observed cost for every observation, we compute averages of both quantities over space and time.

4 Experiments

We consider 50 member ensemble forecasts from IFS ENS and Arches for the year 2021 for 2 meter temperature and 10 meter windspeed with lead times up to 15 days and a horizontal resolution of 1.5° . We use the IFS analysis (IFS HRES fc0) and ERA5 (Hersbach et al., 2020) as ground truth observations for IFS ENS and ArchesweatherGen respectively. All data is available in the Weatherbench dataset (Rasp et al., 2024), except for ArchesweatherGen forecasts, which are obtained by running the trained public model. For each task we compare standard calibration results (see Appendix B for an introduction) to decision calibration results.

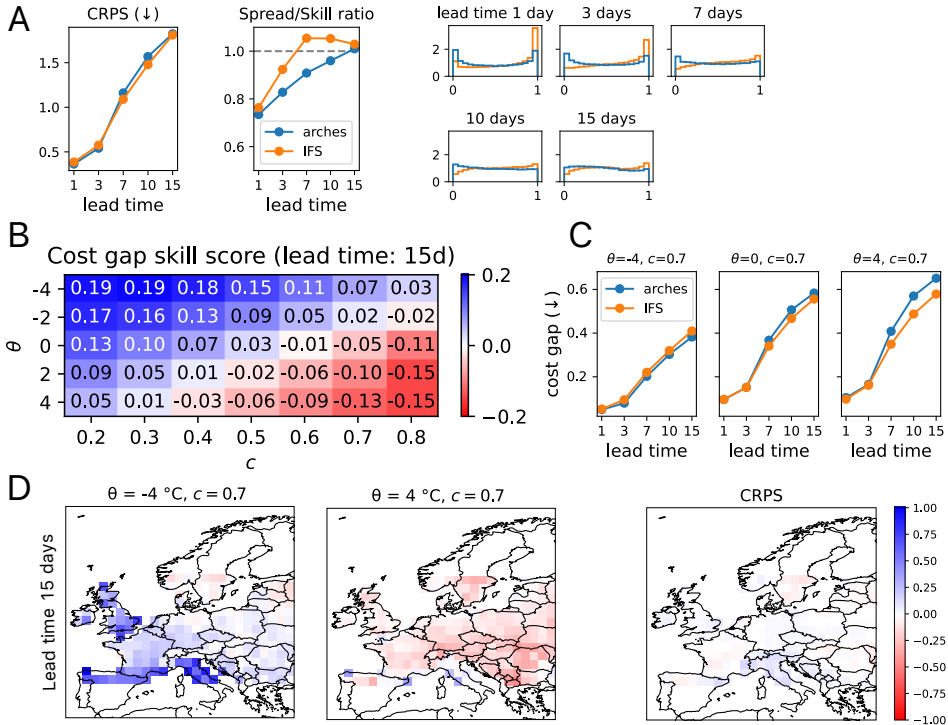


Figure 2: Frost protection task. (A) Results for standard calibration analysis (2 meter temperature) indicate similar performance between both models (particularly for 15 days lead time). (B-D) Results for decision calibration analysis show how cost gap improvements vary across tasks. (B) and (D) show relative improvements (Arches over IFS), where 0.1 means 10% improvement.

4.1 Frost crop protection

CRPS results for 2 meter temperature (00 UTC) indicate similar performance between both models, with Arches performing slightly worse for 7 and 10 days lead time (see Figure 2). SSR results indicate a stronger underdispersion for Arches and some overdispersion for IFS for longer lead times. The PIT histograms indicate similar performance for

lead times longer than 3 days. However, when we consider the frost protection task results (Figure 2 B-D), we can see that decision calibration (cost gap) improvements of Arches over IFS ENS vary across tasks. For low threshold temperatures (θ) Arches yields a better decision calibration than IFS, but as θ increases this effect weakens or even reverses. We observe a similar effect for the cost ratio c . This makes sense as small (large) values of c effectively move the decision boundary of the task further towards lower (higher) temperatures. We see a similar trend for observed costs - improvements in decision calibration generally also lead to lower costs (see Figure C.1). This result highlights the importance of task-dependent evaluations - even small changes in the task can lead to different conclusions about model performance. An effect that goes unnoticed with global calibration metrics.

4.2 Civil heat protection

Both CRPS and PIT histogram results indicate similar calibration performance of both models for 2 meter temperature (12 UTC). SSR results indicate a slightly stronger underdispersion for Arches (see Figure 3). However, for the decision task, we observe a similar pattern as in the frost protection task: different tasks lead to different conclusions about model performance (see Figure 3 B - D). Decision calibration in Arches improves for higher temperatures, often surpassing IFS ENS for high temperatures (θ). We see a similar (but less pronounced) pattern for the observed costs (see Figure C.2). By plotting decision calibration improvement per grid point, we see that model rankings also vary across geographical regions - an effect that can be lost through the aggregation over space. In the mediterranean, Arches performs better than in central Europe; this effect strengthens for higher temperatures.

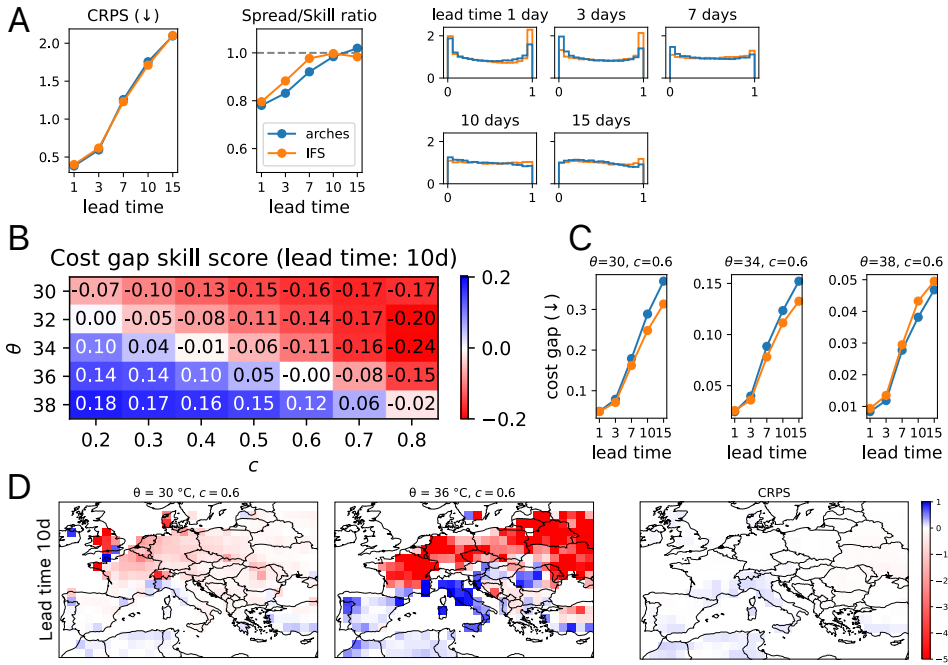


Figure 3: Heat protection task. (A) Results for standard calibration analysis (for 2 meter temperature) indicate similar performance between both models. (B-D) Results for decision calibration analysis show that cost gap improvements vary across tasks. (B) and (D) show relative improvements (Arches over IFS), where 0.1 means 10% improvement.

4.3 Wind power dispatch management

We report standard calibration results for wind speeds.⁴ Both CRPS and PIT histogram suggest very similar performance between Arches and IFS (Figure 4) except for 1 day lead time, where both diagnostics disagree: IFS attains a better CRPS score but a worse PIT histogram that suggests a slight overestimation of wind speeds. SSR results indicate a slight underdispersion for Arches and overdispersion for IFS. The decision calibration analysis reveals only small cost gap differences between both models that vary in strength and direction across lead times (see Figure 4 B-D). Additionally, we find only small differences in the observed costs, with Arches performing slightly better than IFS, see Figure C.4. With increasing penalties, cost gaps decrease for longer lead times. This is because for long lead times we

⁴We consider the wind power transformation to be part of the task.

observe larger forecast uncertainties, so the 'shut-off' action often has the lowest expected cost and since it has constant cost, the cost gap is trivially 0. For some lead times we obtain opposite rankings for cost gap and observed costs. We conjecture that this is due to aggregation effects (over multiple actions) and limited sample size. Wind power trading happens mostly on the day-ahead market, so 1 day lead time performance is most relevant for this task. At this lead time, we see that for CRPS and SSR, Arches performs slightly worse than IFS. Yet, for decision calibration, Arches improves over IFS for stronger penalties, obtaining a lower cost gap (see also Figure 4 D for improvements per grid point). From an economic perspective, Arches is the better model since it yields lower observed costs. Even though the differences are small, the absolute savings can still be significant for larger revenue volumes. We conjecture that the small differences to CRPS rankings are due to the fact that the particular cost function in this example requires decisions across the whole domain and errors are punished similarly for all actions. In this case, decision calibration essentially probes for calibration on a global level (and not on a subset of the domain) and thus model rankings deviate less from those obtained through standard calibration analyses, like CRPS.

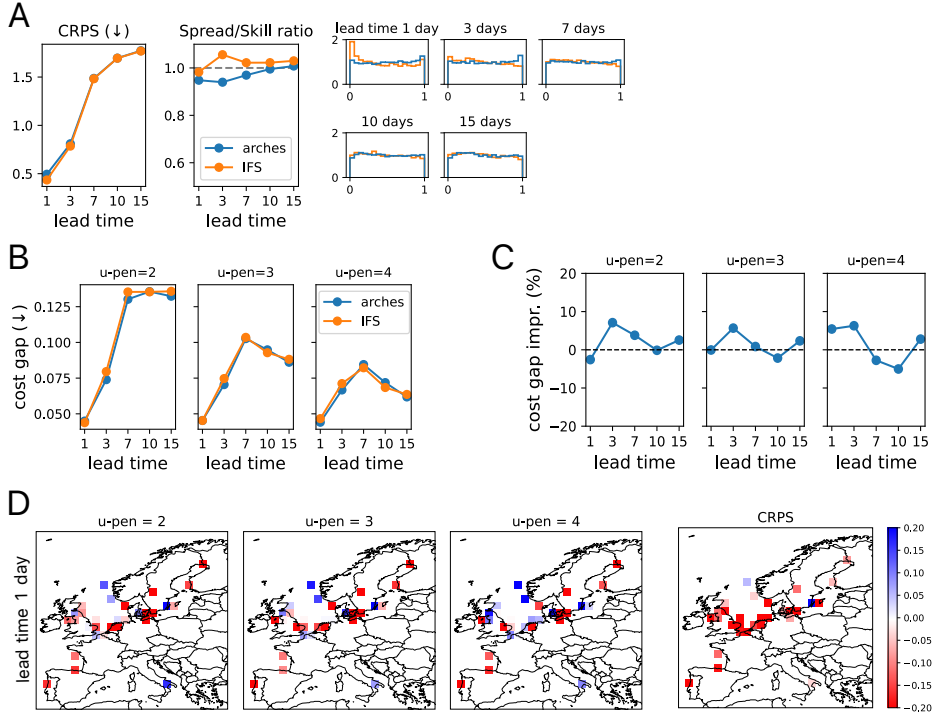


Figure 4: Wind power task. (A) Results for standard calibration analysis and (B-D) decision calibration analysis. (C) and (D) show relative improvements of cost gap (Arches over IFS). (D) shows relative improvement per grid point, where 0.1 means 10% improvement.

5 Conclusion

In this work, we apply the novel framework of decision calibration for weather forecast evaluations. Our results show that performance on typical calibration metrics does not reliably translate into decision-making performance. In a frost protection task, model rankings for decision calibration vary across seemingly similar tasks. In a heat protection task, differences between models only emerge when evaluating calibration at the decision level, demonstrating that decision calibration elegantly assesses forecast calibration for tail events. In a wind power dispatch task we only observe small differences in decision calibration and observed costs between both models. Nonetheless, the small relative differences can lead to large absolute cost savings in large wind farms. We conjecture that decision calibration rankings deviate less from global calibration rankings when cost functions require decisions across the entire output space and errors are punished similarly across actions. One limitation of decision calibration is the requirement of well-defined cost functions, which may not be readily available in practice. Nevertheless, our results highlight the need to evaluate forecast performance at the decision level to identify the best model for a particular decision task. Decision calibration, therefore, offers a promising direction for tailored, task-specific probing of forecast performance. Future work could optimize MLWP models for specific downstream decision tasks by utilizing cost functions as loss function during training or fine-tuning.

References

Abbes, M. and Belhadj, J. (2012). Wind resource estimation and wind park design in el-kef region, tunisia. *Energy*, 40(1):348–357.

Bonev, B., Kurth, T., Mahesh, A., Bisson, M., Kossaifi, J., Kashinath, K., Anandkumar, A., Collins, W. D., Pritchard, M. S., and Keller, A. (2025). Fourcastnet 3: A geometric approach to probabilistic machine-learning weather forecasting at scale. *arXiv preprint arXiv:2507.12144*.

Botterud, A., Zhou, Z., Wang, J., Bessa, R. J., Keko, H., Sumaili, J., and Miranda, V. (2011). Wind power trading under uncertainty in lmp markets. *IEEE Transactions on power systems*, 27(2):894–903.

Bourry, F., Juban, J., Costa, L., and Kariniotakis, G. (2008). Advanced strategies for wind power trading in short-term electricity markets. In *European Wind Energy Conference & Exhibition EWEC 2008*, pages 8–pages. EWEC.

Bruninx, M., Verstraeten, T., Kazempour, J., and Helsen, J. (2025). Day-ahead bidding strategies for wind farm operators under a one-price balancing scheme. In *Proceedings of the 16th ACM International Conference on Future and Sustainable Energy Systems*, pages 719–726.

Calanca, P., Bolius, D., Weigel, A. P., and Liniger, M. A. (2011). Application of long-range weather forecasts to agricultural decision problems in europe. *The Journal of Agricultural Science*, 149(1):15–22.

Chen, L., Zhong, X., Zhang, F., Cheng, Y., Xu, Y., Qi, Y., and Li, H. (2023). Fuxi: a cascade machine learning forecasting system for 15-day global weather forecast. *npj climate and atmospheric science*, 6(1):190.

Couairon, G., Singh, R., Charantonis, A., Lessig, C., and Monteleoni, C. (2024). Archesweather & archesweathergen: a deterministic and generative model for efficient ml weather forecasting. *arXiv preprint arXiv:2412.12971*.

da Silva, M. H. F., de Jesus, G. F., Nascimento, C., da Silva, V. L., and Cruz, C. (2025). Exploring quantum machine learning for weather forecasting. *arXiv preprint arXiv:2509.01422*.

Derr, R., Finocchiaro, J., and Williamson, R. C. (2025). Three types of calibration with properties and their semantic and formal relationships. *arXiv preprint arXiv:2504.18395*.

Dirkson, A. and Buehner, M. (2025). Are we misdiagnosing ensemble forecast reliability? on the insufficiency of spread-error and rank-based reliability metrics. *arXiv preprint arXiv:2512.02160*.

Eriksen, C., Hauri, A., Aebi, S., and Kamberaj, J. (2023). Adapting to climate change: Lessons for swiss civil protection. Technical report, ETH Zurich.

Farkas, H., Linsenmeier, M., Talevi, M., Avner, P., Jafino, B. A., and Sidibe, M. (2025). The economic value of weather forecasts.

Fortin, V., Abaza, M., Anctil, F., and Turcotte, R. (2014). Why should ensemble spread match the rmse of the ensemble mean? *Journal of Hydrometeorology*, 15(4):1708–1713.

Gneiting, T., Balabdaoui, F., and Raftery, A. E. (2007). Probabilistic forecasts, calibration and sharpness. *Journal of the Royal Statistical Society Series B: Statistical Methodology*, 69(2):243–268.

Hersbach, H., Bell, B., Berrisford, P., Hirahara, S., Horányi, A., Muñoz-Sabater, J., Nicolas, J., Peubey, C., Radu, R., Schepers, D., et al. (2020). The era5 global reanalysis. *Quarterly journal of the royal meteorological society*, 146(730):1999–2049.

Hess, J. J., Errett, N. A., McGregor, G., Busch Isaksen, T., Wettstein, Z. S., Wheat, S. K., and Ebi, K. L. (2023). Public health preparedness for extreme heat events. *Annual Review of Public Health*, 44(1):301–321.

Ho, J., Jain, A., and Abbeel, P. (2020). Denoising diffusion probabilistic models. *Advances in neural information processing systems*, 33:6840–6851.

Hughes, S., Bellis, M. A., Bird, W., and Ashton, J. R. (2004). Weather forecasting as a public health tool. *Centre for Public Health, Faculty of Health and Applied Social Sciences*.

Juurakko, C. L., Walker, V. K., et al. (2021). Cold acclimation and prospects for cold-resilient crops. *Plant Stress*, 2:100028.

Lam, R., Sanchez-Gonzalez, A., Willson, M., Wirnsberger, P., Fortunato, M., Alet, F., Ravuri, S., Ewalds, T., Eaton-Rosen, Z., Hu, W., et al. (2023). Learning skillful medium-range global weather forecasting. *Science*, 382(6677):1416–1421.

Lang, S., Alexe, M., Chantry, M., Dramsch, J., Pinault, F., Raoult, B., Clare, M. C., Lessig, C., Maier-Gerber, M., Magnusson, L., et al. (2024a). Aifs–ecmwf’s data-driven forecasting system. *arXiv preprint arXiv:2406.01465*.

Lang, S., Alexe, M., Clare, M. C., Roberts, C., Adewoyin, R., Bouallègue, Z. B., Chantry, M., Dramsch, J., Dueben, P. D., Hahner, S., et al. (2024b). Aifs–crps: ensemble forecasting using a model trained with a loss function based on the continuous ranked probability score. *arXiv preprint arXiv:2412.15832*.

Luber, G. and McGeehin, M. (2008). Climate change and extreme heat events. *American journal of preventive medicine*, 35(5):429–435.

Maciejowska, K., Lipiecki, A., and Uniejewski, B. (2025). Statistical and economic evaluation of forecasts in electricity markets: beyond rmse and mae. *arXiv preprint arXiv:2511.13616*.

Meenal, R., Binu, D., Ramya, K., Michael, P. A., Vinoth Kumar, K., Rajasekaran, E., and Sangeetha, B. (2022). Weather forecasting for renewable energy system: a review. *Archives of Computational Methods in Engineering*, 29(5):2875–2891.

Meerow, S. and Keith, L. (2022). Planning for extreme heat: A national survey of us planners. *Journal of the American Planning Association*, 88(3):319–334.

Murphy, A. H. (1993). What is a good forecast? an essay on the nature of goodness in weather forecasting. *Weather and forecasting*, 8(2):281–293.

Murphy, A. H. (1994). Assessing the economic value of weather forecasts: an overview of methods, results and issues. *Meteorological Applications*, 1(1):69–73.

Palmer, T. (2019). The ecmwf ensemble prediction system: Looking back (more than) 25 years and projecting forward 25 years. *Quarterly Journal of the Royal Meteorological Society*, 145:12–24.

Palmer, T., Molteni, F., Mureau, R., Buizza, R., Chapelet, P., and Tribbia, J. (1993). Ensemble prediction. In *Proc. ECMWF Seminar on Validation of models over Europe*, volume 1, pages 21–66. European Centre for Medium-Range Weather Forecasts Reading, United Kingdom.

Price, I., Sanchez-Gonzalez, A., Alet, F., Andersson, T. R., El-Kadi, A., Masters, D., Ewalds, T., Stott, J., Mohamed, S., Battaglia, P., et al. (2023). Gencast: Diffusion-based ensemble forecasting for medium-range weather. *arXiv preprint arXiv:2312.15796*.

Rasp, S., Hoyer, S., Merose, A., Langmore, I., Battaglia, P., Russell, T., Sanchez-Gonzalez, A., Yang, V., Carver, R., Agrawal, S., et al. (2024). Weatherbench 2: A benchmark for the next generation of data-driven global weather models. *Journal of Advances in Modeling Earth Systems*, 16(6):e2023MS004019.

Richardson, D. S. (2000). Skill and relative economic value of the ecmwf ensemble prediction system. *Quarterly Journal of the Royal Meteorological Society*, 126(563):649–667.

Sahoo, R., Zhao, S., Chen, A., and Ermon, S. (2021). Reliable decisions with threshold calibration. *Advances in Neural Information Processing Systems*, 34:1831–1844.

Snyder, R. L. and Melo-Abreu, J. P. (2005). *Frost protection: fundamentals, practice and economics. Volume 1*, volume 1. Fao.

Sol, B. (1994). Economic impact of weather forecasts for forest fires. *Meteorological Applications*, 1(2):155–158.

Song, H., Diethe, T., Kull, M., and Flach, P. (2019). Distribution calibration for regression. In *International Conference on Machine Learning*, pages 5897–5906. PMLR.

Sweeney, C., Bessa, R. J., Browell, J., and Pinson, P. (2020). The future of forecasting for renewable energy. *Wiley Interdisciplinary Reviews: Energy and Environment*, 9(2):e365.

Wang, Y., Hu, Q., Li, L., Foley, A. M., and Srinivasan, D. (2019). Approaches to wind power curve modeling: A review and discussion. *Renewable and Sustainable Energy Reviews*, 116:109422.

White, G. F. and Haas, J. E. (1975). *Assessment of Research on Natural Hazards*. MIT Press, Cambridge, MA.

Zhao, S., Kim, M., Sahoo, R., Ma, T., and Ermon, S. (2021). Calibrating predictions to decisions: A novel approach to multi-class calibration. *Advances in Neural Information Processing Systems*, 34:22313–22324.

Zhu, Y., Toth, Z., Wobus, R., Richardson, D., and Mylne, K. (2002). The economic value of ensemble-based weather forecasts. *Bulletin of the American Meteorological Society*, 83(1):73–84.

Appendix

A Decision Tasks

A.1 Wind power dispatch management

We extrapolate 10 meter wind speeds (v_{10}) to turbine hub height (h) wind speeds (v_h) using the power law (Abbes and Belhadj, 2012)

$$v_h = v_{10} \cdot \left(\frac{h}{10}\right)^\alpha,$$

with an exponent $\alpha = 0.1$ (accounting for low offshore surface roughness) and hub height $h = 120\text{m}$. We further transform wind speeds into wind power using a standard wind power curve (Figure A.1) using a cubic polynomial curve modeling approach (Wang et al., 2019). We set the cut-in wind speed (v_{in}) to 3 m/s, the rated wind speed (v_{rated}) to 13 m/s and the cut-off wind speed (v_{off}) to 23 m/s.

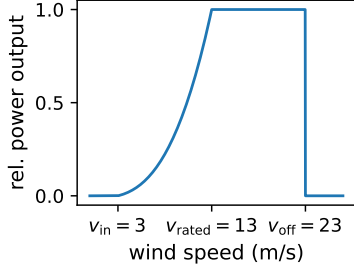


Figure A.1: Wind power curve used to convert wind speed into wind power.

B Calibration diagnostics in weather forecasting

Calibration of weather forecasts is typically verified using the following diagnostic tools. PIT histograms (Gneiting et al., 2007) are used to assess the (rather weak) notion of probabilistic calibration. The probability integral transform (PIT) is obtained by evaluating the predictive CDF at the observation and probabilistic calibration holds when the PIT values follow a uniform distribution. However, probabilistic calibration is rather weak as it only measures forecast calibration on average (over all forecasts) and so no statements can be made about the calibration of individual forecast or even subsets of forecasts. The continuous ranked probability score (CRPS) (Gneiting et al., 2007) is a (strictly) proper scoring rule that quantifies the quality of a probabilistic forecast via a numerical score. Strictly proper scoring rules consider both calibration and sharpness of a forecast and are uniquely minimized if and only if the forecast distribution aligns with the true data generating distribution. The CRPS provides a stronger diagnostic tool than the PIT histogram and is widely employed in the assessment of probabilistic weather forecasts. Finally, the spread-skill ratio (SSR) checks the assumption of exchangeability of the observation and the ensemble members of the forecast to assess calibration (Fortin et al., 2014). It is given by the ratio of the average ensemble spread and the ensemble skill (RMSE of ensemble mean). Intuitively, forecast spread should be a predictor of the skill of the ensemble mean. An SSR of 1.0 is ideal with smaller (larger) values corresponding to underdispersed (overdispersed) ensemble forecasts. Similar to the PIT histogram, the SSR compares spread and skill marginally so conclusions about individual forecast performance can not be drawn. It is important to highlight that both PIT histogram flatness as well as SSR values close to 1.0 are only necessary but insufficient conditions for well-calibrated forecasts, in the sense of distribution calibration (Dirkson and Buehner, 2025).

C Experiments

C.1 Frost Crop Protection

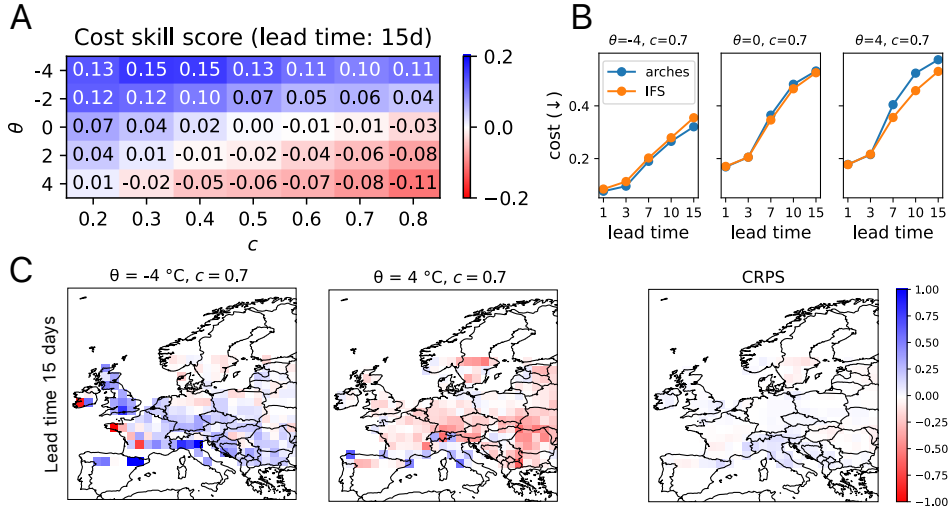


Figure C.1: Frost protection task: Observed costs comparison. (A) and (C) show relative improvements of Arches over IFS (0.1 means 10% improvement).

C.2 Heat Protection

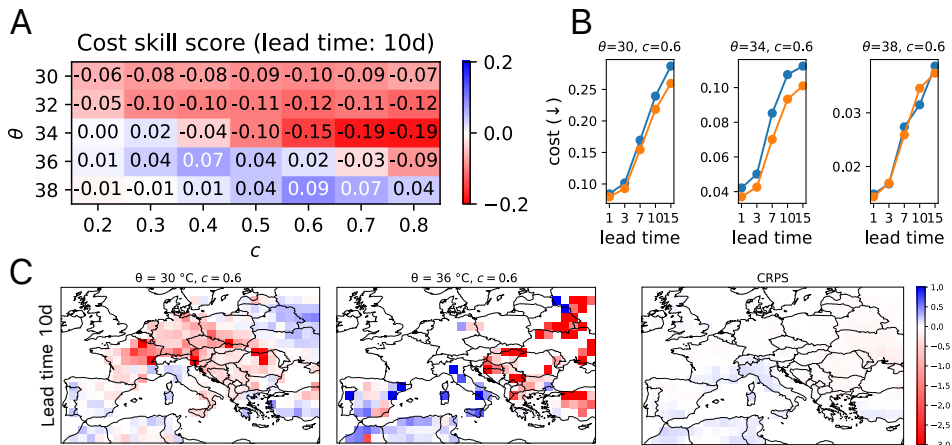


Figure C.2: Heat protection task: Observed costs comparison. (B) shows absolute costs (Arches in blue, IFS in orange). (A) and (C) show relative improvements of Arches over IFS (0.1 means 10% improvement). (C) For $\theta = 36^\circ\text{C}$ many grid points in central Europe show no differences between both models. At those grid points, temperatures are not high enough; hence both models choose the 'no protection' action and obtain the same costs.

C.3 Wind Power Management

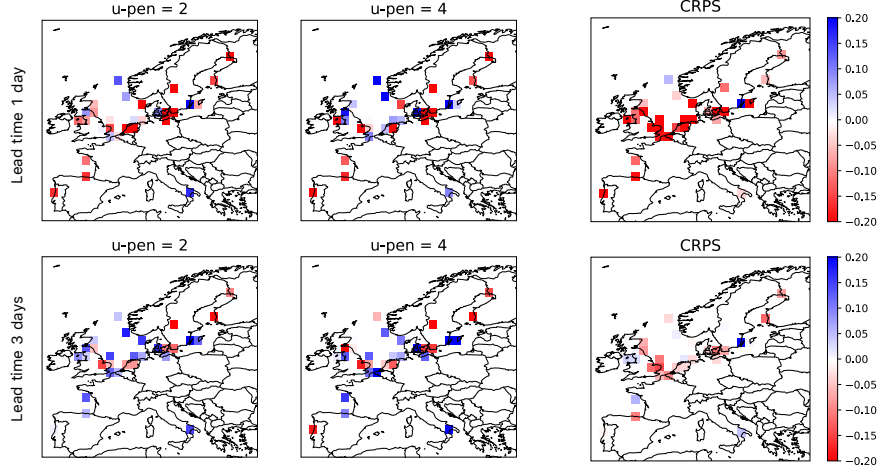


Figure C.3: Wind power management task: relative improvements of cost gap and CRPS (Arches over IFS) per grid point. At 1 day lead time, we see improvements in decision calibration for larger penalties ($u\text{-pen} = 4$). For 3 days lead time, differences to the CRPS ranking are more pronounced and similar across tasks.

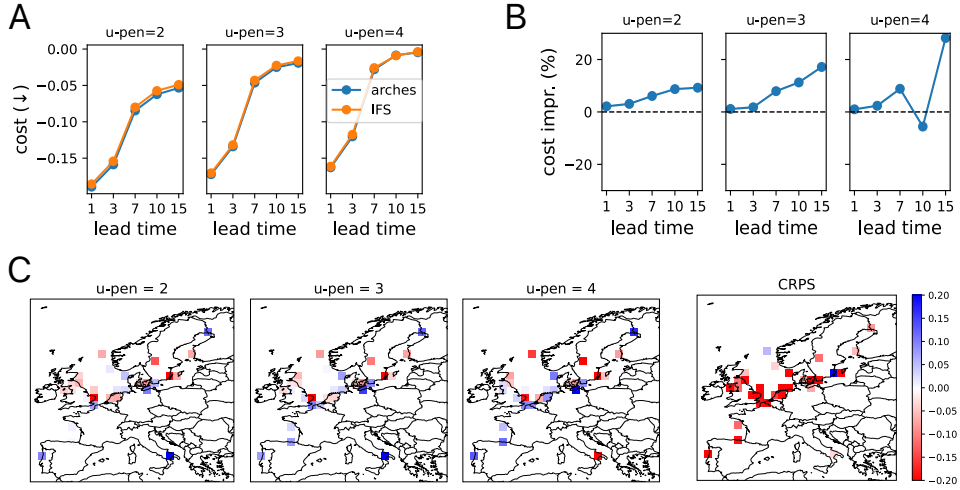


Figure C.4: Wind power management task: Observed cost comparison. (A) We see slightly lower observed costs for Arches across lead times and tasks. (B) Relative improvements of observed costs (Arches over IFS). (C) Relative improvements per grid point for observed costs and CRPS, 0.1 means 10% improvement.